Structure-Activity Analysis of Biased Agonism at the Human Adenosine A$_3$ Receptor

Jo-Anne Baltos, Silvia Paoletta, Anh TN Nguyen, Karen J. Gregory, Dilip K. Tosh, Arthur

Christopoulos, Kenneth A. Jacobson, and Lauren T. May

Drug Discovery Biology, Monash Institute of Pharmaceutical Sciences and Department of

Pharmacology, Monash University, Parkville, VIC 3052, Australia (J.B., A.T.N., K.J.G., A.C.,

L.T.M); and Molecular Recognition Section, Laboratory of Bioorganic Chemistry, National

Institute of Diabetes and Digestive and Kidney Disease, National Institutes of Health, Bethesda,

Maryland 20892, USA (S.P., D.K.T., K.A.J)

Corresponding Author

To whom correspondence should be addressed:

Lauren T. May

Drug Discovery Biology and Department of Pharmacology,

Monash Institute of Pharmaceutical Sciences,

Monash University,

399 Royal Parade, Parkville,

VIC 3052, Australia,

Tel.:(613) 9903-9095

Fax: (613) 9903-9581

E-mail: lauren.may@monash.edu

Manuscript information:

- Number of:
  - Text pages: 21
  - Tables: 3
  - Figures: 6
  - References: 53

- Number of words in:
  - Abstract: 157
  - Introduction: 749
  - Discussion: 1495

Abbreviations

A_3AR, A_3 adenosine receptor; A_3-FlpIn-CHO, Chinese hamster ovary FlpIn™ cells stably expressing the human A_3AR; AB-MECA, N^6-(4-aminobenzyl)-9-[5-(methylcarbonyl)-β-D-ribofuranosyl]adenine; ADA, adenosine deaminase; ANOVA, analysis of variance; AR, adenosine receptor; AT_1R, angiotensin II receptor type 1; ATP, adenosine triphosphate; BSA, bovine serum albumin; cAMP, 3′,5′-cyclic adenosine monophosphate; CCPA, 2-chloro-N^6-cyclopentyladenosine; Cl-IB-MECA, 2-chloro-N^6-(3-iodobenzyl)-adenosine-5′-N-methyluronamide; DBXRM, 1,3-dibutylxanthine-7-riboside-5′-N-methylcarboxamide; DMEM, Dulbecco's Modified Eagle Medium; ERK1/2, extracellular signal-regulated kinases 1 and 2; FBS, fetal bovine serum; GPCR, G protein-coupled receptor; HEMADO, 2-(1-hexynyl)-N-methyladenosine; HEPES, 4-(2-hydroxyethyl)-1-piperazineethanesulfonic acid; IB-MECA, N^6-(3-iodobenzyl)adenosine-5′-N-methyluronamide; MRS542, 2-chloro-N^6-(3-iodobenzyl)adenosine; NECA, 5′-(N-ethylcarboxamido)adenosine; pAkt1/2/3, Akt1/2/3 phosphorylation; pERK1/2, extracellular signal-regulated kinases 1 and 2 phosphorylation; SAR, structure-activity relationship; SEM, standard error of the mean; TM, transmembrane domain.

Abstract

Biased agonism at G protein-coupled receptors (GPCRs) has significant implications for current drug discovery, but molecular determinants that govern ligand bias remain largely unknown. The adenosine A_3 GPCR (A_3AR) is a potential therapeutic target for various conditions, including cancer, inflammation and ischemia, but for which biased agonism remains largely unexplored. We now report the generation of bias "fingerprints" for prototypical ribose containing A_3AR agonists and rigidified (N)-methanocarba 5′-N-methyluronamide nucleoside derivatives with regards to their ability to mediate different signaling pathways. Relative to the reference prototypical agonist IB-MECA, (N)-methanocarba 5′-N-methyluronamide nucleoside derivatives with significant N^6 and/or C2 modifications, including elongated aryl-ethynyl groups, exhibited biased agonism. Significant positive correlation was observed between the C2 substituent length (in Å) and bias towards cell survival. Molecular modeling suggests that extended C2 substituents on (N)-methanocarba 5′-N-methyluronamide nucleosides promotes a progressive outward shift of the A_3AR transmembrane domain 2, which may contribute to the subset of A_3AR conformations stabilized upon biased agonist binding.

Introduction

The A_3 adenosine receptor (A_3AR) belongs to the adenosine family of rhodopsin-like G protein-coupled receptors (GPCRs) (Fredholm et al., 2011). The A_3AR represents a novel therapeutic target for a number of pathologies (Jacobson and Gao, 2006; Fishman et al., 2012). Given their clinical potential, significant effort has been invested into identifying potent A_3AR ligands with high subtype selectivity and minimal species variability (Jacobson et al., 2009; Müller and Jacobson, 2011). Currently two A_3AR agonists, N^6-(3-iodobenzyl)adenosine-5′-N-methyluronamide (IB-MECA) and 2-chloro-N^6-(3-iodobenzyl)-adenosine-5′-N-methyluronamide (Cl-IB-MECA), are in clinical trials for the treatment of psoriasis, rheumatoid arthritis, dry-eye syndrome and hepatocellular carcinoma (Fishman et al., 2012).

GPCRs are dynamic proteins that can adopt a spectrum of conformations (Vaidehi and Kenakin, 2010). Biased agonism results from different agonists stabilizing distinct subsets of GPCR conformations, each associated with their own signaling profile (Kenakin, 2011). Hallmarks of biased agonism include changes in the relative potency of a set of compounds across different signaling pathways, which can result in a reversal in the rank orders of potency or maximal effects (Urban et al., 2006; Kenakin et al., 2012). Although relatively unexplored, A_3AR biased agonism and biased allosteric modulation has been observed at the A_3AR (Gao and Jacobson, 2008; Gao et al., 2011; Verzijl and IJzerman, 2011). Previous studies, which profiled structurally distinct A_3AR ligands in terms of 3′,5′-cyclic adenosine monophosphate (cAMP) accumulation and β-arrestin recruitment, identified compounds that differed with respect to their coupling to G protein-dependent and G protein-independent pathways (Gao and Jacobson, 2008). For example, while the xanthine-7-riboside agonist 1,3-dibutylxanthine-7-riboside-5′-N-methylcarboxamide (DBXRM) had higher efficacy for cAMP accumulation compared to β-arrestin recruitment, the

adenosine derivatives 2-chloro-N^6-cyclopentyladenosine (CCPA) and 2-chloro-N^6-(3-iodobenzyl)adenosine (MRS542) had no significant effect on cAMP accumulation but were partial agonists for β-arrestin recruitment.

Therapeutically, biased agonism can have significant implications, as different signaling patterns may engender divergent clinical outcomes. A well-documented example of this phenomenon occurs at the angiotensin II receptor type 1 (AT_1R). AT_1R antagonists are utilized for treatment of hypertension but are associated with reduced cardiac output (Violin et al., 2010). A biased peptide analogue of angiotensin, Sar-Arg-Val-Tyr-Ile-His-Pro-D-Ala-OH, can reduce blood pressure whilst improving cardiac output through strong activation of β-arrestin recruitment in the absence of G protein signal transduction (Violin et al., 2010; Boerrigter et al., 2011). This example highlights the importance of understanding intracellular signaling profiles in order to both retrospectively and prospectively predict the clinical efficacy of a compound.

The structure-activity relationship (SAR) of A_3AR agonists has been investigated extensively (Jacobson et al., 2009). The affinity and/or subtype selectivity of A_3AR agonists can be enhanced through substitution of the ribose tetrahydrofuryl group with a rigid bicyclo[3.1.0]hexane (methanocarba) ring system, the addition of *m*-substituted benzyl groups at the N^6 position or addition of alkyn-2-yl groups to the C2 position (Kim et al., 1994; Jacobson et al., 2000; Volpini et al., 2009; Tosh et al., 2012a). The North (N)-methanocarba ring system maintains conformation of the ribose ring that is favored at the A_3AR. Furthermore, the subtype selectivity of A_3AR agonists can be enhanced through 5′-N-methyluronamide substitution (Tosh et al., 2012b). Collectively, these studies provide a valuable framework, particularly with respect to the N^6 and C2 position, for the rational design of potent A_3AR agonists with high efficacy and subtype selectivity. However, a limitation of many A_3AR SAR studies is that agonist potency has

been defined using a single assay of receptor function. Such an approach is used routinely within drug discovery to rapidly screen and rank compound libraries according to potency, but is limited with respect to identification of the full spectrum of agonist behaviours and how the SAR relates to biased agonism.

Compounds that represent different chemical space compared to that of the endogenous agonist have a greater propensity to engage and stabilize unique receptor conformations. Given the considerable structural differences between prototypical adenosine receptor (AR) ligands and the A_3AR-selective (N)-methanocarba derivatives, we hypothesized that these compounds may have a biased agonist profile relative to a reference A_3AR agonist. The present study has quantified the bias profile of a number of prototypical A_3AR agonists (Fig. 1) alongside a series of (N)-methanocarba 5′-N-methyluronamide nucleoside derivatives with modifications at the N^6 and C2 position (Fig. 2). Furthermore, the current study explored the SAR of the (N)-methanocarba derivatives with respect to their bias profile, thereby aiding the rational design of future biased A_3AR agonists. We attribute the observed biased agonism favoring cytoprotection to the C2 group extension from the orthosteric binding pocket toward transmembrane domain (TM) 2, which in turn stabilizes a different subset of A_3AR conformations.

Materials and methods

Materials. Fluo-4, Dulbecco's Modified Eagle Medium (DMEM) and Penicillin-Streptomycin were purchased from Invitrogen (Carlsbad, CA). Adenosine deaminase (ADA) and hygromycin-B were purchased from Roche (Basel, Switzerland). Fetal Bovine Serum (FBS) was purchased from ThermoTrace (Melbourne, Australia). AlphaScreen™ SureFire™ extracellular signal-regulated kinases 1 and 2 (ERK1/2), Akt 1/2/3 and cAMP kits were from PerkinElmer (Boston, MA). All compounds prefixed with 'MRS' were synthesized as described previously (Tosh, et al., 2012a; Tosh, et al., 2012b; Toti et al., 2014). All other reagents were purchased from Sigma-Aldrich (St. Louis, MO).

Cell culture. The sequence of the human A_3AR was cloned into the Gateway entry vector, pDONR201, and then transferred in the Gateway destination vector, pEF5/ FRT/V5-dest, using methods described previously (Stewart et al., 2009). A_3-FlpIn-CHO cells were generated using methods described previously (May et al., 2007) and maintained at 37°C in a humidified incubator containing 5% CO_2 in DMEM supplemented with 10% FBS and the selection antibiotic hygromycin-B (500 μg/mL). For cell survival, ERK1/2 phosphorylation, Akt 1/2/3 phosphorylation and calcium mobilization assays, cells were seeded into 96-well culture plates at a density of 4×10^4 cells/well. After 6 h, cells were washed with serum free DMEM and maintained in serum free DMEM for 12 - 18 h at 37°C in 5% CO_2 before assaying. For cAMP assays, cells were seeded into 96-well culture plates at a density of 2×10^4 cells/well and incubated overnight at 37°C in 5% CO_2 prior to assay.

Cell survival assays. Media was removed and replaced with HEPES-buffered saline solution (10 mM 4-(2-hydroxyethyl)-1-piperazineethanesulfonic acid (HEPES), 146 mM NaCl, 10 mM d-glucose, 5 mM KCl, 1mM $MgSO_4$, 1.3 mM $CaCl_2$, and 1.5 mM $NaHCO_3$, pH 7.45) containing

ADA (1 U/mL) and Penicillin-Streptomycin (0.05 U/mL) in the absence and presence of A_3AR ligands. Plates were then maintained at 37°C in a humidified incubator for 24 h, after which 5 µg/ml propidium iodide was added to cells. Plates were then read on an EnVision plate reader (PerkinElmer; Boston, MA), with excitation and emission set to 320 nm and 615 nm, respectively. Data were normalized to 100% cell survival and 0% cell survival, determined at t = 0 h in HEPES buffer and t = 24 h in Milli-Q water, respectively.

ERK1/2 and Akt 1/2/3 phosphorylation assays. A concentration-response curve of ERK1/2 and Akt 1/2/3 phosphorylation for each ligand was performed in serum-free DMEM containing 1 U/mL ADA (5 min exposure at 37°C). Agonist stimulation was terminated by removal of media and addition of 100 µl *SureFire* lysis buffer to each well. Plates were then agitated for 5 min. Detection of pERK1/2 involved an 80:20:120:1:1 v/v/v/v/v dilution of Lysate: Activation Buffer: Reaction Buffer: AlphaScreen acceptor beads: AlphaScreen donor beads in a total volume of 11 µl in a 384-well Proxiplate. Plates were incubated in the dark at 37°C for 1 h followed by measurement of fluorescence by an EnVision plate reader (PerkinElmer; Boston, MA) with excitation and emission set to 630 nm and 520-620 nm, respectively. Detection of Akt 1/2/3 phosphorylation, involved a 40:9.8:39.2:1 v/v/v/v dilution of lysate: activation buffer: reaction buffer: AlphaScreen acceptor beads in a total volume of 9 µl in a 384-well Proxiplate. Plates were incubated in the dark at room temperature for 2 h, after which a 19:1 v/v dilution of dilution buffer: AlphaScreen donor beads was added in a total volume of 11 µl. Plates were incubated at room temperature for a further 2 h followed by measurement of fluorescence by an EnVision plate reader (PerkinElmer; Boston, MA) with excitation and emission set to 630 nm and 520-620 nm, respectively. Agonist concentration-response curves were normalized to the phosphorylation mediated by 10% FBS (5 min stimulation).

Calcium mobilization assays. Media was removed from 96-well plates and replaced with HEPES-buffered saline solution containing 1 U/mL ADA, 2.5 mM probenecid, 0.5% bovine serum albumin (BSA) and 1 µM Fluo4. Plates were incubated in the dark for 1 h at 37°C in a humidified incubator. A FlexStation plate reader (Molecular Devices, Sunnyvale, CA, USA) performed the addition of HEPES-buffered saline solution in the absence and presence of agonist and measured fluorescence (excitation, 485 nm; emission, 520 nm) every 1.52 sec for 75 sec. The difference between the peak and baseline fluorescence was measured as a marker for intracellular Ca^{2+} mobilization. A_3AR agonist concentration-response curves were normalized to the response mediated by 100 µM adenosine triphosphate (ATP) to account for differences in cell number and loading efficiency.

Inhibition of cAMP accumulation assays. Media was replaced with a stimulation buffer (140 mM NaCl, 5 mM KCl, 0.8 µM $MgSO_4$, 0.2 mM Na_2HPO_4, 0.44 mM KH_2PO_4, 1.3 mM $CaCl_2$, 5.6 mM d-glucose, 5 mM HEPES, 0.1% BSA, 1 U/mL ADA and 10 µM rolipram, pH 7.45) and incubated at 37°C for 1 h. Inhibition of cAMP accumulation was assessed by pre-incubation of A_3-FlpIn-CHO cells with A_3AR agonists for 10 min, after which 3 µM forskolin was added for a further 30 min. The reaction was terminated by rapid removal of buffer and addition of 50 µl ice-cold 100% ethanol. Ethanol was allowed to evaporate prior to addition of 50 µl detection buffer (0.1% BSA, 0.3% Tween-20, 5mM HEPES, pH 7.45). Plates were agitated for 10 min, after which 10 µl of lysate was transferred to a 384-well Optiplate. Detection involved addition of a 5 µl 1:49 v/v dilution of AlphaScreen acceptor beads: stimulation buffer. Following this, a 15 µl 1:146:3 v/v/v dilution of AlphaScreen donor beads: detection buffer: 3.3 U/µL biotinylated cAMP to form a total volume of 30 µl. The donor bead/biotinylated cAMP mixture was equilibrated for 30 min prior to addition. Plates were incubated overnight in the dark at room

temperature, followed by measurement of fluorescence by an EnVision plate reader (PerkinElmer; Boston, MA) with excitation and emission set to 630 nm and 520-620 nm, respectively. Agonist concentration-response curves were normalized to the response mediated by 3 μM forskolin (0%) or buffer (100%) alone.

Molecular Modeling. Docking simulations were performed for all the compounds investigated in this study at homology models of the human A_3AR (Data Supplement 1 - 3). In particular, three previously reported models were used: a model entirely based on an agonist-bound $hA_{2A}AR$ crystal structure (PDB code 3QAK), a model based on a hybrid $A_{2A}AR$-β_2 adrenergic receptor template, and a model based on a hybrid $A_{2A}AR$-opsin template (β_2 adrenoceptor X-ray structure PDB ID: 3SN6; opsin crystal X-ray crystal structure PDB ID: 3DQB) (Tosh, et al., 2012a). Models based on hybrid templates show an outward movement of TM2 compared to the $A_{2A}AR$-based model. Structures of A_3AR ligands were built and prepared for docking using the Builder and the LigPrep tools implemented in the Schrödinger suite (Schrödinger Release 2013-3, Schrödinger, LLC, New York, NY, 2013). Molecular docking of the ligands at the A_3AR models was performed by means of the Glide package part of the Schrödinger suite. In particular, a Glide Grid was centered on the centroid of some key residues of the binding pocket of adenosine receptors, namely Phe (EL2), Asn (6.55), Trp (6.48) and His (7.43). The Glide Grid was built using an inner box (ligand diameter midpoint box) of 14 Å x 14 Å x 14 Å and an outer box (box within which all the ligand atoms must be contained) that extended 25 Å in each direction from the inner one. Docking of ligands was performed in the rigid binding site using the XP (extra precision) procedure. The top scoring docking conformations for each ligand were subjected to visual inspection and analysis of protein-ligand interactions to select the proposed binding conformations in agreement with the experimental data.

Data analysis. Statistical analyses and curve fitting were performed using Prism 6 (GraphPad Software, San Diego, CA). To quantify signaling bias, agonist concentration-response curves were analyzed by nonlinear regression using a derivation of the Black-Leff operational model of agonism, as described previously (Kenakin et al., 2012; Wootten et al., 2013; van der Westhuizen et al., 2014). The transduction coefficient, τ/K_A (expressed as a logarithm, $\text{Log}(\tau/K_A)$), was used to quantify biased agonism. In order to account for cell-dependent effects on agonist response, the transduction ratio was normalized to the values obtained for the reference agonist, IB-MECA, to generate $\Delta\text{Log}(\tau/K_A)$. To determine the bias for each agonist at different signaling pathways, the $\Delta\text{Log}(\tau/K_A)$ was normalized to a reference pathway, pERK1/2, to generate $\Delta\Delta\text{Log}(\tau/K_A)$. Bias is defined as $10^{\Delta\Delta\text{Log}(\tau/K_A)}$ where a lack of bias will result in values that are not statistically different from 1, or 0 when expressed as a logarithm. All results are expressed as the mean ± standard error of the mean (SEM). Statistical analyses involved an F test or a one-way analysis of variance (ANOVA) with a Tukey or Dunnett's post-hoc test as referred to within results, with statistical significance determined as $p < 0.05$.

Results

Agonist-mediated signal transduction in FlpIn-CHO cells stably expressing the human A$_3$AR. Quantification of agonist function at multiple intracellular signaling pathways is a requirement to investigate biased agonism. The A$_3$AR preferentially couples to G$_{i/o}$ proteins and therefore agonist activation stimulates the canonical signal transduction pathway, inhibition of adenylate cyclase activity (Fredholm et al., 2001). However, in addition to G$_{i/o}$-adenylate cyclase coupling, A$_3$ARs can also modulate a number of additional G protein-dependent and G protein-independent intracellular signaling pathways (Schulte and Fredholm, 2002; Fossetta et al., 2003; Merighi et al., 2006; Gao and Jacobson, 2008). In this study, agonists were assessed for their ability to inhibit cAMP accumulation, phosphorylate ERK1/2 and Akt(Ser473) 1/2/3, increase intracellular calcium concentrations and promote cytoprotection. Previous studies have established that the (N)-methanocarba derivatives used within the current study have low nanomolar affinity for the high-affinity G protein-coupled state of the human A$_3$AR with the exception of the pyrene containing compounds, MRS5704 and MRS5783 (Fig. 2), which have affinities in the micromolar range (Tosh, et al., 2012a; Tosh, et al., 2012b). Furthermore previous studies have demonstrated that, with the exception of MRS5704 and MRS5776, these compounds confer an equivalent level of inhibition of cAMP accumulation to the non-selective AR agonist 5′-(N-ethylcarboxamido)adenosine (NECA) and therefore are high efficacy agonists at the human A$_3$AR (Tosh, et al., 2012a; Tosh, et al., 2012b).

A concentration-dependent inhibition of 3 μM forskolin stimulated cAMP accumulation in Chinese hamster ovary FlpIn cells stably expressing the human A$_3$AR (A$_3$-FlpIn-CHO) was observed for the prototypical A$_3$AR agonists, IB-MECA, 2-(1-hexynyl)-*N*-methyladenosine (HEMADO), NECA and N[6]-(4-aminobenzyl)-9-[5-(methylcarbonyl)-β-D-ribofuranosyl]adenine

(AB-MECA) (Table 1; Supplemental Fig. 1A), the (N)-methanocarba 5′-N-methyluronamide N^6-(3-chlorobenzyl) nucleoside derivatives with different C2 substituents, i.e. MRS3558, MRS5655, MRS5679, MRS5698, MRS5704 and MRS5783 (Table 1; Supplemental Fig. 1B), and the (N)-methanocarba 5′-N-methyluronamide nucleoside derivatives with additional N^6 modifications, i.e. MRS5667, MRS5857, MRS5916, MRS7030 and MRS7034 (Table 1; Supplemental Fig. 1C). Compared to the reference agonist, IB-MECA, each compound behaved as a full agonist (Table 2). Robust concentration-dependent increases in ERK1/2 phosphorylation (pERK1/2, Table 1; Supplemental Fig. 2) and Akt 1/2/3 phosphorylation (Table 1; Supplemental Fig. 3) were observed for prototypical A_3AR agonists and (N)-methanocarba 5′-N-methyluronamide nucleoside derivatives. When compared to the reference agonist IB-MECA, the majority of agonists behaved as full agonists with the exception of MRS5655, MRS5916, MRS7030 and MRS7034, which stimulated a partial response for pERK1/2, and AB-MECA, MRS5679 and MRS5916, which stimulated a partial response for Akt 1/2/3 phosphorylation (Table 2). A concentration-dependent increase in intracellular calcium mobilization was observed for each agonist assessed (Table 1; Supplemental Fig. 4). Full agonism was observed for the majority of agonists, with the exception of MRS5679, which behaved as a partial agonist (Table 2). Endogenously expressed A_3ARs can promote the survival of a number of different cell types (Matot et al., 2006; Headrick and Lasley, 2009; Fishman et al., 2013). In our heterologous expression system, the ability of A_3AR agonists to increase cell viability after 24 h serum starvation was assessed using propidium iodide, which stains the nuclear matter of cells with a compromised plasma membrane (Kepp et al., 2011). A_3-FlpIn-CHO cell viability was decreased by approximately 40% after 24 h serum starvation. Exposure of cells to either prototypical A_3AR agonists or the (N)-methanocarba 5′-N-methyluronamide nucleoside derivatives mediated a

robust concentration-dependent increase in cell survival, increasing the percentage of viable cells from 60% to approximately 85% (Table 1; Table 2; Supplemental Fig. 5). A similar maximal effect to the reference agonist IB-MECA was observed for each agonist assessed with the exception of MRS5916, MRS7030 and MRS7034 that mediated a partial response, increasing cell survival to approximately 75% (Table 2).

The 4′-truncated (N)-methanocarba derivative MRS5776 has previously been suggested to act as a low efficacy partial agonist (Tosh, et al., 2012b). Consistent with these findings, at signaling pathways assessed in the current study, MRS5776 stimulated either no detectable response (Akt 1/2/3 phosphorylation and calcium mobilization) or behaved as a weak partial agonist (inhibition of cAMP accumulation, ERK1/2 phosphorylation and cell survival) (Table 1; Table 2).

Biased signaling profile of A$_3$AR ligands. The concept of biased agonism arose from experimentally observed variations in the relative potency or maximal effect upon stimulation of different intracellular signaling pathways in a manner that could not be explained by simple differences in the coupling efficiency of intracellular effectors within a particular cell background (Kenakin et al., 2012). A number of changes in the relative potency, and indeed the rank order of potency, were observed for the (N)-methanocarba 5′-N-methyluronamide nucleoside derivatives relative to the reference agonist, IB-MECA (Table 1). The rank order of potency of the reference agonist IB-MECA was ERK1/2 phosphorylation > inhibition of cAMP accumulation > cell survival > Akt 1/2/3 phosphorylation = calcium mobilization (Fig. 3A). In contrast, the highest potency for C2 extended compound MRS5679, relative to all other signaling pathways assessed, was cell survival (Fig. 3B). Furthermore, the N[6] modified compound MRS7034 had a similar potency for inhibition of cAMP accumulation and cell survival, but lower potency for ERK1/2 phosphorylation, Akt 1/2/3 phosphorylation and calcium mobilization

(Fig. 3C). These are two examples of changes in relative potencies causing a change in the rank order of agonist potency. For two compounds, differential partial agonism across the different signaling endpoints was observed. The N^6 unsubstituted compound, MRS5916, is a partial agonist for stimulating ERK1/2 phosphorylation and cell survival but a full agonist with respect to calcium mobilization (Table 2). In contrast, N^6 substituted MRS5679, which is highly extended with a biarylethynyl group at C2, is a partial agonist for stimulating calcium mobilization but a full agonist for ERK1/2 phosphorylation and cell survival (Fig. 3B; Table 2). Collectively, these results demonstrate that a number of the (N)-methanocarba 5′-N-methyluronamide nucleoside derivatives display biased agonism relative to the reference agonist IB-MECA.

An extension to the Black-Leff operational model was used to quantify bias (Kenakin et al., 2012). Transduction coefficients, $Log(\tau/K_A)$, for each ligand at each pathway assessed were estimated from concentration-response data. To account for system bias, the $Log(\tau/K_A)$ value was normalized to the reference agonist IB-MECA, to generate $\Delta Log(\tau/K_A)$ (Table 3). In order to minimize the propagation of error, statistical analysis interrogating significant differences in the signaling was assessed using the $\Delta Log(\tau/K_A)$ value. Relative to IB-MECA, the prototypical agonists NECA, HEMADO and AB-MECA display no significant bias at any of the pathways assessed (Fig. 4A). In contrast, a number of compounds in the (N)-methanocarba series exhibit significant bias at one or more of the pathways investigated. With the exception of MRS3558, each of the (N)-methanocarba 5′-N-methyluronamide N^6-(3-chlorobenzyl) nucleoside derivatives had significant bias towards cell survival relative to at least one other pathway (Fig. 4B). The bias profile for the (N)-methanocarba 5′-N-methyluronamide nucleoside derivatives with additional N^6 modifications was more complex, with compounds possessing bias towards cell

survival, away from calcium mobilization and/or towards cAMP accumulation (Fig. 4C). The effect of 4′-truncation on signaling bias was not determined as MRS5776 had minimal activity at the majority of signaling intermediates assessed (Table 2).

The $\Delta Log(\tau/K_A)$ values were then normalized to a reference pathway, pERK1/2, to generate $\Delta\Delta Log(\tau/K_A)$ values (Table 3). In addition to accounting for the system bias, the $\Delta\Delta Log(\tau/K_A)$ value, referred to hereafter as the Log(bias factor), also accounts for differences in agonist efficacy. To better conceptualize and visualize the data, bias factors were plotted on a 'web of bias'. The 'web of bias' clearly demonstrates that, relative to IB-MECA, the prototypical agonists NECA, HEMADO and AB-MECA display no bias as evidenced by each of the values approximating to 1 (Fig. 5A). In contrast, a number of compounds in the (N)-methanocarba series exhibit bias towards cell survival, away from calcium mobilization and/or towards the inhibition of cAMP accumulation (Fig. 5, B and C). Collectively, these data establish that a number of the conformationally constrained (N)-methanocarba 5′-N-methyluronamide nucleoside derivatives have significant bias, relative to IB-MECA, and suggest that one or more of their distinct structural features may have a role in promoting the divergent signaling profile observed.

To assess the SAR of the bias profiles, the length (in Å) of the C2 and N^6 substituents of the (N)-methanocarba 5′-N-methyluronamide nucleoside derivatives were compared to the bias detected. The bias conferred upon varying the N^6 substituent was complex and no clear relationship was evident. In contrast, there was a significant positive relationship between the length of the C2 substituent and the cell survival Log(bias factor) for compounds with an N^6-(3-chlorobenzyl) substituent (r^2= 0.92, p<0.05). That is, increasing the length of the C2 substituent increased the bias towards cell survival (Fig. 5D). Importantly, A₃AR ligands had no effect on cell survival in

non-transfected FlpIn-CHO cells, confirming that the bias identified was downstream of the A_3AR (Supplemental Fig. 6). As such, these data have identified a key constituent on (N)-methanocarba 5′-N-methyluronamide nucleoside derivatives that can promote bias at the A_3AR towards increased cell survival.

Docking into A_3AR Homology Models. Molecular modeling was used to facilitate the understanding of the relationship between the length of the C2 substituent and bias observed at the A_3AR. To date, there are no available crystallographic structures of the human A_3AR. However, several crystal structures of the human $A_{2A}AR$ in complex with both agonists and antagonists have been reported (Jaakola et al., 2008; Xu et al., 2011; Doré et al., 2011), highlighting the key interactions for ligand binding at the adenosine receptor family. Previous studies have suggested that homology models of the human A_3AR, based on the human $A_{2A}AR$, cannot accommodate (N)-methanocarba substituted compounds with rigid elongated C2 substituents in an orientation that would form key interactions with residues of the binding site. Instead, docking of such derivatives required models based on a hybrid $A_{2A}AR$-β_2 adrenergic receptor template or a hybrid $A_{2A}AR$-opsin template where TM2 is shifted outward from the binding site (Tosh et al., 2012a). Similarly, in the present study these hybrid models were used to dock the (N)-methanocarba 5′-N-methyluronamide nucleoside derivatives with extended C2 substituents (Data Supplement 1 - 3). In particular, MRS3558 fit the A_3AR model based entirely on the human $A_{2A}AR$, MRS5655 and MRS5698 required the hybrid $A_{2A}AR$-β_2 receptor model, while MRS5679, MRS5704 and MRS5783 required the hybrid $A_{2A}AR$-opsin model (Fig. 6). Therefore, the extension of the C2 substituent seems to be correlated with a progressive shift of TM2 outward from the binding site that is likely to promote the stabilization of a unique subset of A_3AR conformations responsible for biased activation.

The effect of the C2 substituent on receptor conformation seems to be modulated also by the N^6 group of the ligand. This substituent is accommodated in a mainly hydrophobic region delimited by the second extracellular loop and can have an effect in determining the overall conformation of the receptor explaining why the bias pattern changes for compounds bearing the same C2 group but different N^6 substituents. Furthermore, the (N)-methanocarba ring of the studied nucleoside derivatives forces the pseudo-sugar moiety into a North-envelope conformation and thereby constrains the orientation of the interactions with key residues in the lower part of the binding site, including Thr94 in TM3 and Ser271 and His272 in TM7, known to be important in receptor activation (interactions not formed in antagonist-bound structures) (Jaakola et al., 2008; Xu et al., 2011). This constrained conformation could also be responsible for the bias of (N)-methanocarba derivatives, relative to the reference agonist IB-MECA.

Discussion

The emerging paradigm of GPCR biased agonism has become an increasingly important concept in modern drug discovery. The SAR of biased agonism has been investigated previously at a number of GPCRs, including the β_2 adrenergic and dopamine D_2 receptors (Holloway et al., 2002; Chen et al., 2012; Shonberg et al., 2013). However, bias at the A_3AR remains a relatively new concept (Gao and Jacobson, 2008). The current study took advantage of the rich SAR surrounding the A_3AR to gain insights into the structural determinants that govern bias at this receptor. We investigated the signaling profile of a series of (N)-methanocarba substituted derivatives, which have a relatively rigid conformation, in addition to prototypical A_3AR agonists, and correlated the observed patterns with proposed structural plasticity of the A_3AR (Tosh et al., 2012). Relative to the reference agonist IB-MECA, the prototypical A_3AR agonists NECA, HEMADO and AB-MECA, which all contain flexible ribose rings, did not display biased signaling at any of the five signaling pathways investigated. In contrast, a number of the structurally distinct (N)-methanocarba derivatives displayed significant bias, relative to IB-MECA, for cell survival signaling, intracellular calcium mobilization and/or inhibition of cAMP accumulation. Moreover, this study has identified the C2 group of (N)-methanocarba 5′-N-methyluronamide nucleoside agonists as a key determinant for signaling bias towards cell survival.

As there is no X-ray crystallographic structure of the A_3AR, homology modeling of the human A_3AR can facilitate the interpretation of SAR studies for (N)-methanocarba nucleosides. Within the $A_{2A}AR$ crystal structure, non-conserved disulphide bonds constrain the extracellular portion of TM2 towards the TM bundle (Tosh et al., 2012). However, docking of rigid (N)-methanocarba

5′-N-methyluronamide nucleoside derivatives with elongated C2 substituents at the A_3AR model required a significant outward movement of TM2 to maintain conserved polar contacts surrounding the ribose and adenine moieties. As such, these compounds were better accommodated using a hybrid $A_{2A}AR-\beta_2$ adrenergic receptor template or an $A_{2A}AR$-opsin template, which have an approximate 4 Å and 7 Å outward movement of the extracellular portion of TM2 at the Ca atom of Ser73, respectively (Tosh et al., 2012). These findings highlight the significant conformational changes that are likely to occur upon binding of biased A_3AR agonists.

Although residues of TM2 are not predicted to be directly involved in binding of prototypical A_3AR agonists, this transmembrane domain has been suggested previously to play an important role in modulating ligand binding and receptor activation. Mutagenesis studies at the A_1AR and A_3AR suggest residues within TM2 govern the negative allosteric modulation observed for sodium on agonist binding (Barbhaiya et al., 1996; Gao et al., 2003). This hypothesis was recently validated by the high-resolution antagonist-bound $A_{2A}AR$ crystal structure that identified the highly conserved aspartate residue in TM2, $Asp^{2.50}$, as a key residue within the sodium-binding pocket (Liu et al., 2012). Furthermore, TM2 is involved in a water-mediated hydrogen bond network with TM1, TM6 and TM7, which has been suggested to regulate GPCR activation (Rosenkilde et al., 2010; Nygaard et al., 2010). Our data suggest that the altered conformation, stabilized in the presence of rigid (N)-methanocarba 5′-N-methyluronamide nucleoside derivatives with elongated C2 substituents, may contribute to cytoprotective signaling in A_3-FlpIn-CHO cells.

Whilst this study found a clear relationship between C2 length and cell survival, there was no accompanying preferential coupling to the ERK1/2 and Akt 1/2/3 phosphorylation pathways,

which have been implicated in promoting cell survival in a number of settings (Wada and Penninger, 2004; Manning and Cantley, 2007). This suggests that the conformations induced by these ligands may give rise to protective signaling that is independent of these protein kinases and/or represents compartmentalized signaling that was not detected using the methods employed. Of particular interest for future studies would be to investigate the ability of the different classes of ligands to couple to G protein-independent pathways, such as β-arrestin recruitment, as this has been shown to play an important role in A_3AR signaling (Gao and Jacobson, 2008). The ability of A_3AR agonists to stimulate β-arrestin recruitment will also influence subsequent A_3AR desensitization and/or internalization. These time-dependent processes are an important consideration, as signaling assays require different incubations times, and therefore may be differentially influenced by A_3AR desensitization and/or internalization. Future studies will also assess the binding kinetics of structurally distinct A_3AR agonists, as it is becoming appreciated that the agonist residence time can influence the efficacy and bias profile observed (Sykes et al., 2009; Guo et al., 2012; Herenbrink 2016).

This study has found a clear relationship between C2 length of (N)-methanocarba substituted derivatives and ligand bias. However, also of interest is the SAR pertaining to modifications at the N^6 position. MRS5655 and MRS5916 differ only by their N^6 substituent; MRS5655 contains a 3-chlorobenzyl and MRS5916 a primary amine group. Interestingly, while N^6 unsubstituted MRS5916 displayed no significant bias, the corresponding N^6-(3-chlorobenzyl) analogue MRS5655 had significant bias towards cell survival relative to calcium. However, a further elongated N^6 substituent in MRS5857 produced equivalent activities in cell survival and calcium. Similarly, the structures of highly C2-extended MRS5679 and MRS5667 differ only by their N^6 substituents; MRS5679 has a 3-chlorobenzyl group, while MRS5667 has a methyl group. Both

compounds are biased towards cell survival relative to all pathways, however, MRS5667 has additional bias towards cAMP and therefore a slightly different signaling fingerprint to that of MRS5679. The degree of bias can also be influenced by subtle changes in agonist structure. At a qualitative level, the N^6 stereoisomers, MRS7030 and MRS7034, show the same bias profile. However, while MRS7030 has approximately 6-fold bias towards cell survival and cAMP, greater effects are observed for MRS7034, with this compound having approximately 28-fold and 23-fold bias towards cell survival and cAMP, respectively. Collectively, these findings indicate that the N^6 substituent, which interacts with extracellular regions of the A_3AR, is likely to play an important role in driving A_3AR signal transduction and signaling bias. Furthermore, it is clear that the SAR surrounding A_3AR biased agonism is multifactorial and likely to involve interactions with a number of residues within and outside the binding pocket that can be influenced by one or more chemical modifications. Some structural differences did not alter the signaling profile; for example, 1- and 4-pyrene isomers, MRS5704 and MRS5783, respectively, displayed the same profile. The effect of 4′-truncation on signaling bias could not be determined because truncated MRS5776 was inactive at a number of the pathways assessed.

As a pharmacological paradigm, biased agonism can provide significant advantages in situations where both the desired effects and adverse effects are activated downstream of the same target. A_1AR biased agonism has been previously investigated (Langemeijer et al., 2013; Valant et al., 2014; Baltos et al., 2016) and recently demonstrated to allow for the selective stimulation of cardioprotective signal transduction in the absence of the adverse haemodynamic effects commonly associated with A_1AR therapies (Valant et al., 2014). The current study has identified a range of bias profiles for subtype selective A_3AR agonists, which offer a potential therapeutic advantage. Importantly, these bias profiles must be validated in relevant endogenous systems in

order to understand the system-dependence of the signaling fingerprints and therefore better gauge the therapeutic potential. However, if similar bias profiles were observed within the cell type of interest, the discovery of biased cytoprotective compounds may have clinical implications when targeting the A_3AR. A_3AR activation is protective in cardiac and lung ischemia-reperfusion injury and can prevent glaucoma-induced cell death (Matot et al., 2006; Headrick and Lasley, 2009; Fishman et al., 2013). Paradoxically, although low concentrations of A_3AR agonists stimulate pro-survival signaling, high concentrations promote apoptosis (Jacobson, 1998). Therefore, A_3AR agonists that preferentially couple to pro-survival pathways may promote A_3AR-mediated cell survival in the absence of apoptotic signal transduction. The A_3AR is also a potential target for the treatment of hepatocellular carcinoma, with an A_3AR agonist currently in clinical trials (Fishman et al., 2012). In cancerous cells, A_3AR activation promotes apoptosis and decreases proliferation through stimulation of $G_{i/o}$ proteins, which decreases the PKA-mediated inhibition of GSK-3β. GSK-3β destabilizes Wnt signal transduction, an important pathway for proliferation and cell cycle progression (Fishman et al., 2002; Bar-Yehuda et al., 2008). As such, agonists such as MRS5667, MRS7030, and MRS7034, which display bias towards the inhibition of cAMP accumulation, may be of relevance in the treatment of hepatocellular carcinoma.

This study highlights the importance of rigorously assessing the signaling profile of lead compounds intended for future clinical use. High-throughput screening at a single endpoint is necessary for rapid assessment of novel chemical entities; however, this method only provides a snapshot of the full signaling repertoire and therefore is unable to identify biased agonists. Through profiling at multiple signaling pathways, this study has identified a number of A_3AR biased agonists. Furthermore, we have informed, for the first time, the SAR surrounding A_3AR

biased agonism, particularly with respect to the observed bias towards cell survival. An understanding of the SAR involved in conferring A_3AR biased agonism will allow for the rational design of novel A_3AR therapeutics that can fine tune the downstream signal transduction and therefore enhance the observed clinical efficacy.

Acknowledgements

Authorship contributions

Participated in research design: Baltos, Christopoulos, Jacobson, May.

Conducted experiments: Baltos. Paoletta, Nguyen.

Performed data analysis: Baltos, Paoletta, Nguyen.

Wrote or contributed to the writing of the manuscript: Baltos, Paoletta, Gregory, Tosh, Christopoulos, Jacobson, May.

References

Baltos J-A, Gregory KJ, White PJ, Sexton PM, Christopoulos A, and May LT (2016) Quantification of adenosine A_1 receptor biased agonism: Implications for drug discovery. *Biochem Pharmacol* **99**:101–112.

Bar-Yehuda S, Stemmer SM, Madi L, Castel D, Ochaion A, Cohen S, Barer F, Zabutti A, Perez-Liz G, Del Valle L, and Fishman P (2008) The A_3 adenosine receptor agonist CF102 induces apoptosis of hepatocellular carcinoma via de-regulation of the Wnt and NF-kappaB signal transduction pathways. *Int J Oncol* **33**:287–295.

Barbhaiya H, McClain R, Ijzerman A, and Rivkees SA (1996) Site-directed mutagenesis of the human A_1 adenosine receptor: influences of acidic and hydroxy residues in the first four transmembrane domains on ligand binding. *Mol Pharmacol* **50**:1635–1642.

Boerrigter G, Lark MW, Whalen EJ, Soergel DG, Violin JD, and Burnett JC (2011) Cardiorenal actions of TRV120027, a novel β-arrestin-biased ligand at the angiotensin II type I receptor, in healthy and heart failure canines: a novel therapeutic strategy for acute heart failure. *Circ Heart Fail* **4**:770–778.

Chen X, Sassano MF, Zheng L, Setola V, Chen M, Bai X, Frye SV, Wetsel WC, Roth BL, and Jin J (2012) Structure–functional selectivity relationship studies of β-Arrestin-biased dopamine D_2 receptor agonists. *J Med Chem* **55**:7141–7153.

Doré AS, Robertson N, Errey JC, Ng I, Hollenstein K, Tehan B, Hurrell E, Bennett K, Congreve M, Magnani F, Tate CG, Weir M, and Marshall FH (2011) Structure of the adenosine A_{2A} receptor in complex with ZM241385 and the xanthines XAC and caffeine. *Structure*

19:1283–1293.

Fishman P, Bar-Yehuda S, Liang BT, and Jacobson KA (2012) Pharmacological and therapeutic effects of A$_3$ adenosine receptor agonists. *Drug Discov Today* **17**:359–366.

Fishman P, Bar-Yehuda S, Madi L, and Cohn I (2002) A$_3$ adenosine receptor as a target for cancer therapy. *Anticancer Drugs* **13**:437–443.

Fishman P, Cohen S, and Bar-Yehuda S (2013) Targeting the A$_3$ adenosine receptor for glaucoma treatment (review). *Mol Med Rep* **7**:1723–1725.

Fossetta J, Jackson J, Deno G, Fan X, Du XK, Bober L, Soudé-Bermejo A, de Bouteiller O, Caux C, Lunn C, Lundell D, and Palmer RK (2003) Pharmacological analysis of calcium responses mediated by the human A$_3$ adenosine receptor in monocyte-derived dendritic cells and recombinant cells. *Mol Pharmacol* **63**:342–350.

Fredholm BB, IJzerman AP, Jacobson KA, Klotz KN, and Linden J (2001) International union of pharmacology. XXV. Nomenclature and classification of adenosine receptors. *Pharmacol Rev* **53**:527–552.

Fredholm BB, IJzerman AP, Jacobson KA, Linden J, and Müller CE (2011) International Union of Basic and Clinical Pharmacology. LXXXI. Nomenclature and classification of adenosine receptors-an update. *Pharmacol Rev* **63**:1–34.

Gao Z-G, and Jacobson KA (2008) Translocation of arrestin induced by human A$_3$ adenosine receptor ligands in an engineered cell line: comparison with G protein-dependent pathways. *Pharmacol Res* **57**:303–311.

Gao Z-G, Kim S-K, Gross AS, Chen A, Blaustein JB, and Jacobson KA (2003) Identification of essential residues involved in the allosteric modulation of the human A_3 adenosine receptor. *Mol Pharmacol* **63**:1021–1031.

Gao Z-G, Verzijl D, Zweemer A, Ye K, Göblyös A, IJzerman AP, and Jacobson KA (2011) Functionally biased modulation of A_3 adenosine receptor agonist efficacy and potency by imidazoquinolinamine allosteric enhancers. *Biochem Pharmacol* **82**:658–668.

Guo D, Mulder-Krieger T, IJzerman AP, and Heitman LH (2012) Functional efficacy of adenosine A_{2A} receptor agonists is positively correlated to their receptor residence time. *Br J Pharmacol* **166**:1846–1859.

Headrick JP, and Lasley RD (2009) Adenosine receptors and reperfusion injury of the heart. *Handb Exp Pharmacol* 189–214.

Herenbrink CK, Sykes DA, Donthamsetti P, Canals M, Coudrat T, Shonberg J, Scammells PJ, Capuano B, Sexton PM, Charlton SJ, Javitch JA, Christopoulos A, and Lane JR (2016) The role of kinetic context in apparent biased agonism at GPCRs. *Nat Commun* **7**:1–14.

Holloway AC, Qian H, Pipolo L, Ziogas J, Miura S-I, Karnik S, Southwell BR, Lew MJ, and Thomas WG (2002) Side-chain substitutions within angiotensin II reveal different requirements for signaling, internalization, and phosphorylation of type 1A angiotensin receptors. *Mol Pharmacol* **61**:768–777.

Jaakola V-P, Griffith MT, Hanson MA, Cherezov V, Chien EYT, Lane JR, IJzerman AP, and Stevens RC (2008) The 2.6 angstrom crystal structure of a human A_{2A} adenosine receptor bound to an antagonist. *Science* **322**:1211–1217.

Jacobson KA (1998) Adenosine A$_3$ receptors: novel ligands and paradoxical effects. *Trends Pharmacol Sci* **19**:184–191.

Jacobson KA, and Gao Z-G (2006) Adenosine receptors as therapeutic targets. *Nat Rev Drug Discov* **5**:247–264.

Jacobson KA, Ji X-D, Li A-H, Melman N, Siddiqui MA, Shin K-J, Marquez VE, and Ravi RG (2000) Methanocarba analogues of purine nucleosides as potent and selective adenosine receptor agonists. *J Med Chem* **43**:2196–2203.

Jacobson KA, Klutz AM, Tosh DK, Ivanov AA, Preti D, and Baraldi PG (2009) Medicinal chemistry of the A$_3$ adenosine receptor: agonists, antagonists, and receptor engineering. *Handb Exp Pharmacol* 123–159.

Kenakin T (2011) Functional selectivity and biased receptor signaling. *J Pharmacol Exp Ther* **336**:296–302.

Kenakin T, Watson C, Muniz-Medina V, Christopoulos A, and Novick S (2012) A simple method for quantifying functional selectivity and agonist bias. *ACS Chem Neurosci* **3**:193–203.

Kepp O, Galluzzi L, Lipinski M, Yuan J, and Kroemer G (2011) Cell death assays for drug discovery. *Nat Rev Drug Discov* **10**:221–237.

Kim HO, Ji XD, Siddiqi SM, Olah ME, Stiles GL, and Jacobson KA (1994) 2-Substitution of N6-benzyladenosine-5'-uronamides enhances selectivity for A$_3$ adenosine receptors. *J Med Chem* **37**:3614–3621.

Langemeijer EV, Verzijl D, Dekker SJ, and IJzerman AP (2013) Functional selectivity of adenosine A_1 receptor ligands? *Purinergic Signal* **9**:91–100.

Liu W, Chun E, Thompson AA, Chubukov P, Xu F, Katritch V, Han GW, Roth CB, Heitman LH, IJzerman AP, Cherezov V, and Stevens RC (2012) Structural basis for allosteric regulation of GPCRs by sodium ions. *Science* **337**:232–236.

Manning BD, and Cantley LC (2007) AKT/PKB signaling: navigating downstream. *Cell* **129**:1261–1274.

Matot I, Weiniger CF, Zeira E, Galun E, Joshi BV, and Jacobson KA (2006) A_3 adenosine receptors and mitogen-activated protein kinases in lung injury following in vivo reperfusion. *Crit Care* **10**:R65.

May LT, Avlani VA, Langmead CJ, Herdon HJ, Wood MD, Sexton PM, and Christopoulos A (2007) Structure-function studies of allosteric agonism at M_2 muscarinic acetylcholine receptors. *Mol Pharmacol* **72**:463–476.

Merighi S, Benini A, Mirandola P, Gessi S, Varani K, Leung E, MacLennan S, Baraldi PG, and Borea PA (2006) Modulation of the Akt/Ras/Raf/MEK/ERK pathway by A_3 adenosine receptor. *Purinergic Signal* **2**:627–632.

Müller CE, and Jacobson KA (2011) Recent developments in adenosine receptor ligands and their potential as novel drugs. *BBA - Biomembranes* **1808**:1290–1308.

Nygaard R, Valentin-Hansen L, Mokrosinski J, Frimurer TM, and Schwartz TW (2010) Conserved water-mediated hydrogen bond network between TM-I, -II, -VI, and -VII in 7TM

receptor activation. *J Biol Chem* **285**:19625–19636.

Rosenkilde MM, Benned-Jensen T, Frimurer TM, and Schwartz TW (2010) The minor binding pocket: a major player in 7TM receptor activation. *Trends Pharmacol Sci* **31**:567–574.

Schulte G, and Fredholm BB (2002) Signaling pathway from the human adenosine A_3 receptor expressed in Chinese hamster ovary cells to the extracellular signal-regulated kinase 1/2. *Mol Pharmacol* **62**:1137–1146.

Shonberg J, Herenbrink CK, López L, Christopoulos A, Scammells PJ, Capuano B, and Lane JR (2013) A structure–activity analysis of biased agonism at the dopamine D_2 Receptor. *J Med Chem* **56**:9199–9221.

Stewart GD, Valant C, Dowell SJ, Mijaljica D, Devenish RJ, Scammells PJ, Sexton PM, and Christopoulos A (2009) Determination of adenosine A_1 receptor agonist and antagonist pharmacology using Saccharomyces cerevisiae: implications for ligand screening and functional selectivity. *J Pharmacol Exp Ther* **331**:277–286.

Sykes DA, Dowling MR, and Charlton SJ (2009) Exploring the Mechanism of Agonist Efficacy: A Relationship between Efficacy and Agonist Dissociation Rate at the Muscarinic M_3 Receptor. *Mol Pharmacol* **76**:543–551.

Tosh DK, Deflorian F, Phan K, Gao Z-G, Wan TC, Gizewski E, Auchampach JA, and Jacobson KA (2012a) Structure-guided design of A_3 adenosine receptor-selective nucleosides: combination of 2-arylethynyl and bicyclo[3.1.0]hexane substitutions. *J Med Chem* **55**:4847–4860.

Tosh DK, Paoletta S, Phan K, Gao Z-G, and Jacobson KA (2012b) Truncated nucleosides as A_3 adenosine receptor ligands: Combined 2-arylethynyl and bicyclohexane substitutions. *ACS Med Chem Lett* **3**:596–601.

Urban JD, Clarke WP, Zastrow von M, Nichols DE, Kobilka B, Weinstein H, Javitch JA, Roth BL, Christopoulos A, Sexton PM, Miller KJ, Spedding M, and Mailman RB (2006) Functional selectivity and classical concepts of quantitative pharmacology. *J Pharmacol Exp Ther* **320**:1–13.

Vaidehi N, and Kenakin T (2010) The role of conformational ensembles of seven transmembrane receptors in functional selectivity. *Curr Opin Pharmacol* **10**:775–781.

Valant C, May LT, Aurelio L, Chuo CH, White PJ, Baltos JA, Sexton PM, Scammells PJ, and Christopoulos A (2014) Separation of on-target efficacy from adverse effects through rational design of a bitopic adenosine receptor agonist. *Proc Natl Acad Sci USA* **111**:4614–4619.

Van der Westhuizen ET, Breton B, Christopoulos A, and Bouvier M (2014) Quantification of ligand bias for clinically relevant β_2-Adrenergic receptor ligands: implications for drug taxonomy. *Mol Pharmacol* **85**:492–509.

Verzijl D, and IJzerman AP (2011) Functional selectivity of adenosine receptor ligands. *Purinergic Signal* **7**:171–192.

Violin JD, DeWire SM, Yamashita D, Rominger DH, Nguyen L, Schiller K, Whalen EJ, Gowen M, and Lark MW (2010) Selectively engaging β-arrestins at the angiotensin II type 1 receptor reduces blood pressure and increases cardiac performance. *J Pharmacol Exp Ther*

335:572–579.

Volpini R, Buccioni M, Dal Ben D, Lambertucci C, Lammi C, Marucci G, Ramadori AT, Klotz
K-N, and Cristalli G (2009) Synthesis and biological evaluation of 2-Alkynyl- N6-methyl-5′-
N-methylcarboxamidoadenosine derivatives as potent and highly selective agonists for the
human adenosine A$_3$ receptor. *J Med Chem* **52**:7897–7900.

Wada T, and Penninger JM (2004) Mitogen-activated protein kinases in apoptosis regulation.
Oncogene **23**:2838–2849.

Wootten D, Savage EE, Willard FS, Bueno AB, Sloop KW, Christopoulos A, and Sexton PM
(2013) Differential activation and modulation of the glucagon-like peptide-1 receptor by
small molecule ligands. *Mol Pharmacol* **83**:822–834.

Xu F, Wu H, Katritch V, Han GW, Jacobson KA, Gao ZG, Cherezov V, and Stevens RC (2011)
Structure of an agonist-bound human A$_{2A}$ adenosine receptor. *Science* **332**:322–327.

Footnotes

Fig. 1. Structures of the prototypical A_3AR agonists used within this study.

Fig. 2. Investigation of the SAR for biased A_3AR agonists based on (N)-methanocarba derivatives with modified N^6 and C2 groups. The binding affinity for the human A_3AR, determined from $[^{125}I]AB$-MECA membrane binding, is indicated in parentheses (Tosh et al., 2012a; Tosh et al., 2012b).

Fig. 3. (N)-Methanocarba derivatives demonstrate differential signaling profiles relative to the reference agonist, IB-MECA. The signaling profile for the reference agonist, IB-MECA (A), the C2 extended (N)-methanocarba derivative, MRS5679 (B), and the N^6 modified (N)-methanocarba derivative, MRS7034 (C) in A_3-FlpIn-CHO cells. Data points, expressed as a percentage of stimulation by 100 nM IB-MECA for the corresponding pathway, represent the mean $\pm$ SEM of 3 separate experiments conducted in duplicate or triplicate. Error bars not shown lie within the dimensions of the symbol.

Fig. 4. (N)-Methanocarba derivatives display significant bias relative to the reference agonist, IB-MECA. Quantification and statistical analysis of signal bias using $\Delta Log(\tau/K_A)$ values estimated for prototypical A_3AR agonists (A), (N)-methanocarba N^6-(3-chlorobenzyl) derivatives with different C2 substituents (B) and (N)-methanocarba derivatives with different N^6 modifications (C) for ERK1/2 phosphorylation, inhibition of cAMP accumulation, Akt 1/2/3(Ser473) phosphorylation, intracellular calcium mobilization and cell survival in A_3-FlpIn-CHO cells. $*P<0.05$, $**P<0.01$, $***P<0.001$, $****P<0.0001$ one-way ANOVA; Tukey's multiple comparisons. Data points represent the mean $\pm$ SEM of 3-9 separate experiments conducted in duplicate. Error bars not shown lie within the dimensions of the symbol.

Fig. 5. 'Web of bias' for A_3AR agonists. The bias profile of prototypical A_3AR agonists (A), (N)-methanocarba N^6-(3-chlorobenzyl) derivatives with different C2 substituents (B) and (N)-methanocarba derivatives with different N^6 modifications (C) can be visualized on a 'web of bias'. The 'web of bias' plots bias factor for each ligand and for every signaling pathway tested. Bias factors have been normalized to the reference ligand, IB-MECA, and the reference pathway, ERK1/2 phosphorylation. Linear regression analysis (D) identified a significant positive relationship with respect to agonist C2 length (Å) and bias towards cell survival for compounds with an N^6-(3-chlorobenzyl) substituent. Log(bias factor) = $\Delta\Delta$Log(τ/K_A).

Fig. 6. The predicted binding mode of MRS5679, an (N)-methanocarba nucleoside derivative with an extended C2 substituent at the human A_3AR. (A) Docking pose of MRS5679 (red carbon sticks) at the A_3AR model based on a hybrid $A_{2A}AR$-opsin template where TM2 (magenta ribbon) is shifted outward from the binding site. Side chains of residues forming hydrogen bonds with MRS5679 at adenosine receptors are shown in grey carbon sticks. Ligand-receptor H-bonding interactions are pictured as black dotted lines. (B) Comparison of different A_3AR models (top view), showing the outward shift of TM2 (yellow arrow) in the hybrid $A_{2A}AR$-opsin model (blue/magenta ribbon) compared to the model based entirely on the human $A_{2A}AR$ (grey ribbon). The pose of MRS5679 (red carbon sticks) at the A_3AR model based on a hybrid $A_{2A}AR$-opsin template is shown as reference.

Table 1. The potency (pEC_{50}) values of A_3AR agonists for intracellular signaling pathways in A_3-FlpIn-CHO cells.

Data represents the mean ± SEM of 3-9 separate experiments conducted in duplicate or triplicate.

Compound	pERK 1/2	cAMP	pAkt	Ca^{2+}_i	Survival
IB-MECA	9.6 ± 0.1	9.4 ± 0.1	8.9 ± 0.2	8.9 ± 0.4	9.2 ± 0.2
NECA	8.6 ± 0.1	8.3 ± 0.1	7.6 ± 0.2	8.2 ± 0.1	8.3 ± 0.3
HEMADO	9.4 ± 0.1	9.3 ± 0.1	8.1 ± 0.2	9.3 ± 0.2	9.1 ± 0.3
AB-MECA	8.1 ± 0.1	7.6 ± 0.2	7.5 ± 0.2	7.9 ± 0.3	8.1 ± 0.2
MRS3558	9.8 ± 0.1	9.6 ± 0.1	8.8 ± 0.2	8.5 ± 0.3	10.2±0.2
MRS5655	9.3 ± 0.1	9.1 ± 0.1	8.3 ± 0.2	7.5 ± 0.3	9.7 ± 0.2
MRS5667	8.1 ± 0.1	8.5 ± 0.2	8.2 ± 0.1	7.6 ± 0.1	9.9 ± 0.2
MRS5679	7.6 ± 0.1	8.1 ± 0.1	6.6 ± 0.4	6.7 ± 0.4	9.6 ± 0.2
MRS5698	8.1 ± 0.1	8.3 ± 0.1	8.1 ± 0.1	7.8 ± 0.1	9.5 ± 0.2
MRS5704	6.2 ± 0.1	6.7 ± 0.1	5.8 ± 0.1	5.4 ± 0.2	7.9 ± 0.2
MRS5776	7.8 ± 0.1	6.8 ± 0.7	NA	NA	8.3 ± 0.4
MRS5783	6.0 ± 0.1	6.5 ± 0.1	5.9 ± 0.1	5.5 ± 0.1	7.7 ± 0.1
MRS5857	9.7 ± 0.1	9.1 ± 0.1	8.8 ± 0.2	7.7 ± 0.4	9.9 ± 0.2
MRS5916	9.5 ± 0.1	9.5 ± 0.1	9.2 ± 0.1	8.3 ± 0.1	9.5 ± 0.3
MRS7030	8.1 ± 0.1	8.8 ± 0.1	7.9 ± 0.1	7.2 ± 0.1	8.4 ± 0.3
MRS7034	8.0 ± 0.1	9.4 ± 0.1	7.8 ± 0.1	7.6 ± 0.2	9.2 ± 0.2

NA= no detectable response.

Table 2. The maximal effect (E_{MAX}) values of A_3AR agonists for intracellular signaling pathways in A_3-FlpIn-CHO cells.

Data represents the mean $\pm$ SEM of 3-9 experiments conducted in duplicate or triplicate.

Compound	pERK 1/2	cAMP	pAkt	Ca^{2+}_i	Survival
IB-MECA	106 ± 3	72 ± 4	21 ± 1	32 ± 4	85 ± 2
NECA	97 ± 2	80 ± 4	15 ± 1	$50 \pm 2*$	83 ± 3
HEMADO	99 ± 2	75 ± 2	18 ± 2	36 ± 2	82 ± 2
AB-MECA	93.1 ± 4	78 ± 6	$10 \pm 1*$	34 ± 5	81 ± 2
MRS3558	94 ± 4	70 ± 2	19 ± 2	45 ± 5	85 ± 1
MRS5655	$88 \pm 5*$	78 ± 3	24 ± 2	40 ± 5	83 ± 1
MRS5667	112 ± 3	71 ± 6	25 ± 1	43 ± 1	82 ± 1
MRS5679	95 ± 6	59 ± 4	$14 \pm 4*$	$13 \pm 3*$	85 ± 2
MRS5698	106 ± 3	89 ± 4	27 ± 1	46 ± 2	81 ± 1
MRS5704	107 ± 5	70 ± 3	26 ± 1	41 ± 8	79 ± 1
MRS5776	$13 \pm 1*$	$17 \pm 9*$	NA	NA	$71 \pm 2*$
MRS5783	112 ± 5	78 ± 4	21 ± 1	41 ± 2	80 ± 1
MRS5857	102 ± 5	73 ± 4	21 ± 1	34 ± 5	87 ± 1
MRS5916	$81 \pm 3*$	79 ± 2	$12 \pm 1*$	36 ± 1	$76 \pm 2*$
MRS7030	$88 \pm 3*$	80 ± 3	16 ± 1	37 ± 2	$77 \pm 2*$
MRS7034	$89 \pm 3*$	79 ± 1	16 ± 1	36 ± 2	$78 \pm 2*$

*Significantly different, $p<0.05$ (One-way ANOVA, Dunnet's post-hoc), when compared to the E_{MAX} value of IB-MECA at each respective pathway.

NA= no detectable response.

Table 3. Transduction coefficients $(Log(\tau/K_A))$, normalized transduction coefficients $(\Delta Log(\tau/K_A))$ and Log(bias factors) used to quantify biased agonism at the A_3AR.

Data represents the mean $\pm$ SEM of 3-9 separate experiments conducted in duplicate or triplicate.

Compound	Parameter	pERK1/2	cAMP	pAkt	Ca^{2+}_i	Survival
IB-MECA	$Log(\tau/K_A)$	9.5 ± 0.3	9.4 ± 0.1	9.4 ± 0.3	8.6 ± 0.2	9.6 ± 0.2
	$\Delta Log(\tau/K_A)$	0	0	0	0	0
	Log(bias factor)	0	0	0	0	0
	Bias factor	1	1	1	1	1
NECA	$Log(\tau/K_A)$	8.6 ± 0.1	8.5 ± 0.2	8.1 ± 0.3	8.2 ± 0.1	8.4 ± 0.1
	$\Delta Log(\tau/K_A)$	-0.9 ± 0.3	-0.9 ± 0.1	-1.3 ± 0.3	-0.4 ± 0.2	-1.2 ± 0.3
	Log(bias factor)	0	0.1 ± 0.2	-0.4 ± 0.2	0.6 ± 0.3	-0.3 ± 0.3
	Bias factor	1	1.0	0.4	3.6	0.5
HEMADO	$Log(\tau/K_A)$	9.4 ± 0.1	8.8 ± 0.2	8.9 ± 0.1	8.7 ± 0.2	9.2 ± 0.1
	$\Delta Log(\tau/K_A)$	-0.1 ± 0.2	-0.6 ± 0.2	-0.4 ± 0.3	0.1 ± 0.1	-0.4 ± 0.2
	Log(bias factor)	0	-0.5 ± 0.4	-0.3 ± 0.2	0.2 ± 0.2	-0.3 ± 0.2
	Bias factor	1	0.3	0.5	1.7	0.5
AB-MECA	$Log(\tau/K_A)$	8.0 ± 0.1	7.7 ± 0.2	8.0 ± 0.3	7.5 ± 0.2	7.7 ± 0.3
	$\Delta Log(\tau/K_A)$	-1.5 ± 0.3	-1.7 ± 0.2	-1.4 ± 0.1	-1.1 ± 0.1	-1.9 ± 0.6
	Log(bias factor)	0	-0.2 ± 0.4	0.1 ± 0.2	0.4 ± 0.3	-0.4 ± 0.6
	Bias factor	1	0.6	1.2	2.5	0.4
MRS3558	$Log(\tau/K_A)$	9.7 ± 0.2	9.7 ± 0.1	9.4 ± 0.2	8.4 ± 0.2	10.3 ± 0.3
	$\Delta Log(\tau/K_A)$	0.2 ± 0.2	0.3 ± 0.1	-0.1 ± 0.2	-0.2 ± 0.1	0.7 ± 0.4
	Log(bias factor)	0	0.1 ± 0.1	-0.2 ± 0.3	-0.4 ± 0.2	0.5 ± 0.3

	Bias factor	1	1.4	0.6	0.4	3.1
MRS5655	$\text{Log}(\tau/K_A)$	9.0 ± 0.4	9.1 ± 0.1	8.9 ± 0.4	7.4 ± 0.3	9.9 ± 0.2
	$\Delta\text{Log}(\tau/K_A)$	-0.6 ± 0.1	-0.2 ± 0.1	-0.5 ± 0.3	-1.1 ± 0.2	0.3 ± 0.4
	Log(bias factor)	0	0.3 ± 0.1	0.1 ± 0.2	-0.6 ± 0.2	0.9 ± 0.4
	Bias factor	1	2.1	1.1	0.3	8.1
MRS5667	$\text{Log}(\tau/K_A)$	8.2 ± 0.1	8.7 ± 0.1	8.2 ± 0.1	7.6 ± 0.1	9.8 ± 0.1
	$\Delta\text{Log}(\tau/K_A)$	-1.3 ± 0.1	-0.6 ± 0.1	-1.2 ± 0.1	-1.0 ± 0.1	0.2 ± 0.1
	Log(bias factor)	0	0.7 ± 0.2	0.2 ± 0.1	0.3 ± 0.2	1.6 ± 0.1
	Bias factor	1	4.7	1.4	2.0	36
MRS5679	$\text{Log}(\tau/K_A)$	7.3 ± 0.3	7.6 ± 0.3	7.0 ± 0.3	5.9 ± 0.4	9.7 ± 0.2
	$\Delta\text{Log}(\tau/K_A)$	-2.3 ± 0.1	-1.7 ± 0.3	-2.4 ± 0.1	-2.7 ± 0.2	0.1 ± 0.1
	Log(bias factor)	0	0.5 ± 0.4	-0.2 ± 0.2	-0.5 ± 0.3	2.3 ± 0.1
	Bias factor	1	3.2	0.7	0.4	224
MRS5698	$\text{Log}(\tau/K_A)$	8.1 ± 0.1	8.5 ± 0.2	8.1 ± 0.1	7.8 ± 0.1	9.4 ± 0.1
	$\Delta\text{Log}(\tau/K_A)$	-1.4 ± 0.1	-0.9 ± 0.2	-1.2 ± 0.1	-0.7 ± 0.1	-0.1 ± 0.1
	Log(bias factor)	0	0.5 ± 0.3	0.2 ± 0.1	0.7 ± 0.2	1.3 ± 0.1
	Bias factor	1	3.2	1.6	5.0	20
MRS5704	$\text{Log}(\tau/K_A)$	6.2 ± 0.1	6.5 ± 0.1	6.0 ± 0.1	5.3 ± 0.2	7.9 ± 0.4
	$\Delta\text{Log}(\tau/K_A)$	-3.3 ± 0.1	-2.9 ± 0.1	-3.3 ± 0.1	-3.3 ± 0.2	-1.7 ± 0.4
	Log(bias factor)	0	0.4 ± 0.1	-0.1 ± 0.1	0.1 ± 0.2	1.6 ± 0.3
	Bias factor	1	2.6	0.9	1.0	44
MRS5783	$\text{Log}(\tau/K_A)$	6.1 ± 0.1	6.4 ± 0.2	5.9 ± 0.1	5.5 ± 0.1	7.8 ± 0.4
	$\Delta\text{Log}(\tau/K_A)$	-3.4 ± 0.1	-2.9 ± 0.2	-3.5 ± 0.1	-3.1 ± 0.1	-1.8 ± 0.4

	Log(bias factor)	0	0.5 ± 0.1	-0.1 ± 0.1	0.3 ± 0.1	1.6 ± 0.4
	Bias factor	1	3.0	0.8	2.0	43
MRS5857	Log(τ/K$_A$)	9.4 ± 0.5	9.1 ± 0.1	9.3 ± 0.5	7.6 ± 0.3	10.2± 0.2
	ΔLog(τ/K$_A$)	-0.1 ± 0.2	-0.3 ± 0.2	-0.1 ± 0.2	-1.0 ± 0.2	0.6 ± 0.3
	Log(bias factor)	0	-0.2 ± 0.3	0.1 ± 0.1	-0.8 ± 0.4	0.8 ± 0.3
	Bias factor	1	0.7	1.1	0.2	5.9
MRS5916	Log(τ/K$_A$)	9.5 ± 0.1	9.5 ± 0.1	9.2 ± 0.1	8.2 ± 0.1	9.7 ± 0.1
	ΔLog(τ/K$_A$)	-0.1 ± 0.1	0.1 ± 0.1	-0.1 ± 0.1	-0.3 ± 0.1	0.1 ± 0.1
	Log(bias factor)	0	0.1 ± 0.2	-0.1 ± 0.1	-0.3 ± 0.1	0.1 ± 0.1
	Bias factor	1	1.3	0.8	0.5	1.3
MRS7030	Log(τ/K$_A$)	8.2 ± 0.1	8.8 ± 0.2	8.1 ± 0.1	7.2 ± 0.1	9.0 ± 0.1
	ΔLog(τ/K$_A$)	-1.3 ± 0.1	-0.5 ± 0.2	-1.3 ± 0.1	-1.4 ± 0.1	-0.6 ± 0.1
	Log(bias factor)	0	0.8 ± 0.2	0.1 ± 0.1	-0.1 ± 0.1	0.8 ± 0.2
	Bias factor	1	6.3	1.2	1.0	6.2
MRS7034	Log(τ/K$_A$)	8.1 ± 0.2	9.4 ± 0.1	8.1 ± 0.2	7.5 ± 0.1	9.7 ± 0.1
	ΔLog(τ/K$_A$)	-1.4 ± 0.2	0.1 ± 0.1	-1.3 ± 0.2	-1.0 ± 0.1	0.1 ± 0.1
	Log(bias factor)	0	1.4 ±0.2	0.1 ± 0.1	0.3 ± 0.3	1.4 ± 0.1
	Bias factor	1	23.4	1.3	2.1	28

Significance as illustrated in Figure 4

NECA

IB-MECA

HEMADO

AB-MECA
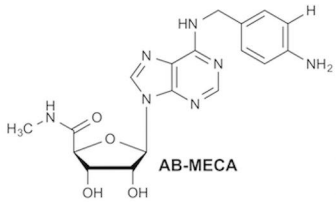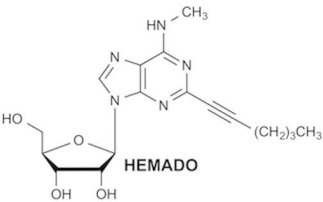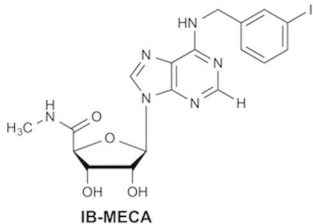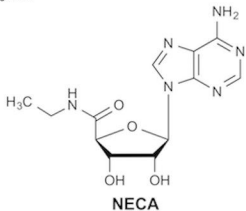
Figure. 2
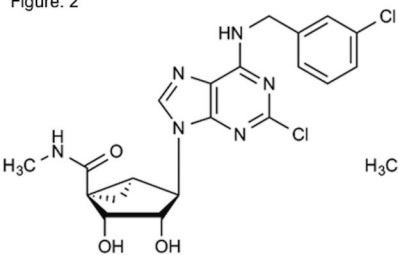
MRS3558 (0.29 nM)
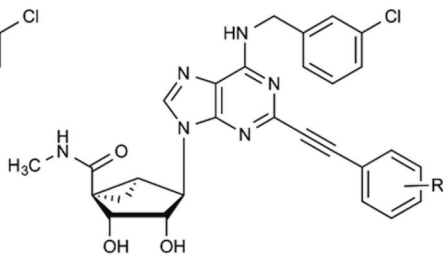
R = H, MRS5655 (1.34 nM)
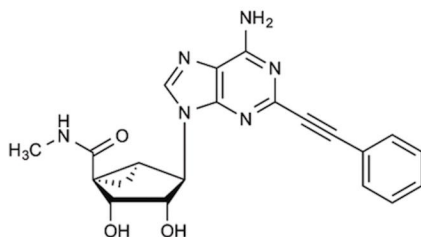
R = 3,4-di-F, MRS5698 (3.49 nM)

R = 4-Ph, MRS5679 (3.06 nM)
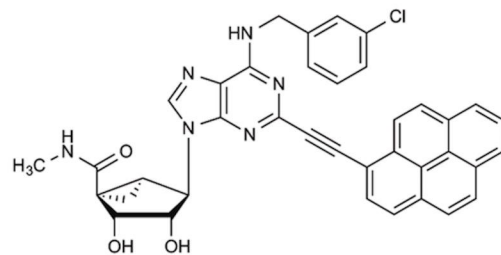
MRS5704 (68.3 nM)
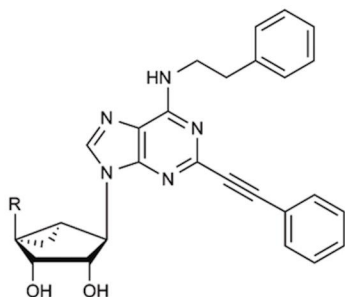
R = H, MRS5776 (20 nM)
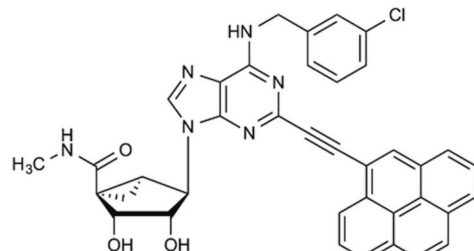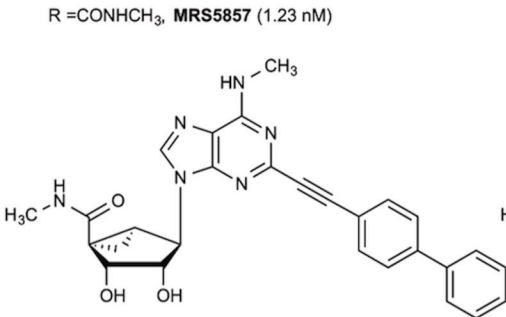
R =CONHCH₃, MRS5857 (1.23 nM)
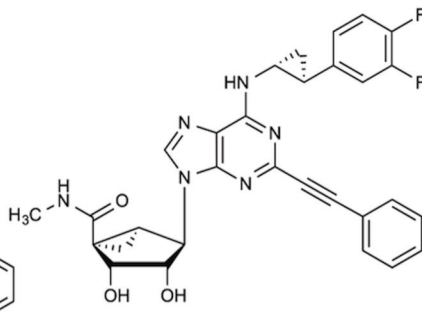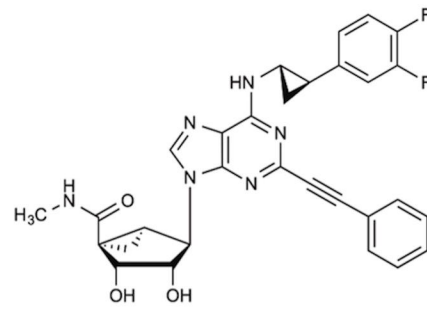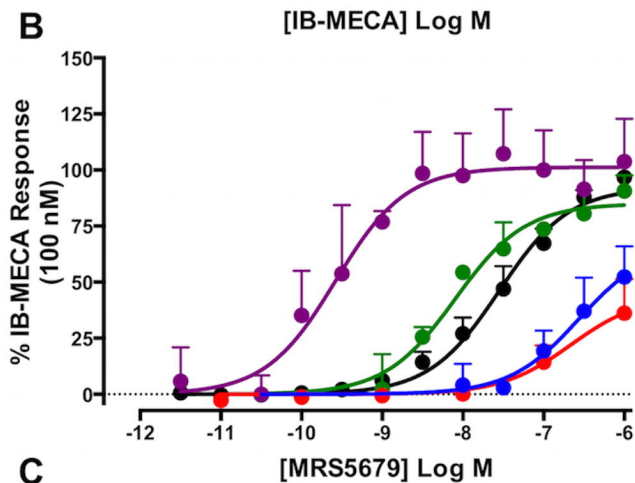
MRS5916 (1.51 nM)

MRS5783 (680 nM)

MRS5667 (3.1 nM)
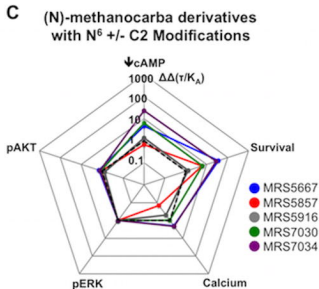
MRS7030 (16.9 nM)

MRS7034 (4.55 nM)

Figure 4

Figure 5

A Prototypical Ligands

↓cAMP
1000 ΔΔ(τ/K_A)
100
10
1
0.1

pAKT · · · · IB-MECA
· HEMADO
· NECA
· AB-MECA
Survival

pERK
Calcium

B (N)-methanocarba derivatives
with C2 Modifications

↓cAMP
1000 ΔΔ(τ/K_A)
100
10
1
0.1

pAKT
Survival
· MRS3558
· MRS5655
· MRS5698
· MRS5783
· MRS5704
· MRS5679

pERK
Calcium

C (N)-methanocarba derivatives
with N[6] +/- C2 Modifications

↓cAMP
1000 ΔΔ(τ/K_A)
100
10
1
0.1

pAKT
Survival
· MRS5667
· MRS5857
· MRS5916
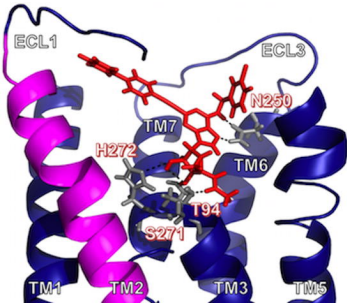· MRS7030
· MRS7034

pERK
Calcium

D Correlation: C2 Length (Å) and
Bias towards Cell Survival

Log Bias (Cell Survival)

· MRS3558
· MRS5655
· MRS5698
· MRS5783
· MRS5704
· MRS5679

C2 Length (Å)

$r^2 = 0.92$

Figure 6

A — ECL1, ECL3, TM7, H272, S271, T94, N250, TM6, TM1, TM2, TM3, TM5

B — ECL2, TM4, TM3, ECL1, TM2, ECL3, TM5, TM6, TM7, TM1